

Neural Networks: A set of four case studies

Stéphane Forsik

1 Introduction

The intention here is to present some practical examples of the application of neural networks. Four cases have been chosen from the published literature. In each, a neural network has been used to establish relations between input parameters and the output parameter to model. Those four cases are:

- Estimation of the amount of retained austenite in austempered ductile irons (M. A. Yescas *et al.* [1]): the volume fraction of retained austenite in ductile irons was analysed and described as a function of the chemical composition and the heat treatment.
- Neural network model of creep strength of austenitic stainless steels (T. Sourmail *et al.* [2]): the 10^4 hours creep rupture stress was analysed and described as a function of the chemical composition and stress parameters.
- Neural-network analysis of irradiation hardening in low-activation steels (R. Kemp *et al.* [3]): the yield strength of irradiated low-activation steels has been analysed and described as a function of the chemical composition, heat treatment and irradiation parameters.
- Application of bayesian neural network for modelling and prediction of ferrite number in austenitic stainless steel welds (M. Vasudevan *et al.* [4]): the ferrite volume fraction in austenitic stainless welds has been analysed and described as a function of the chemical composition.

2 Procedure

In those four cases, the same procedure to build a neural network was always followed. A problem involving complex relations between inputs and outputs was identified. Mechanisms involved in this relation are known and well-described but are too complex to be quantitatively described by proposed models (linear or pseudo-linear relations). Moreover those models do not take in account relations between inputs parameters and are generally not reliable for extrapolation. The use of a neural was in the this case the best solution.

To analyse a problem using a neural network, the procedure generally follows these three steps:

- Compilation of a set of data: after the problem has been identified, appropriate parameters need to be selected. A set of data obtained in experiments already carried out and reported in the literature was compiled and used for the neural network.
- Training and testing of the model: this part is done by the software but improvement can be brought to the database to obtain better models and minimise error bars.
- Predictions: once the best committee has been selected and if it gives satisfactory results, the model is checked and finally ready for predictions.

3 First example: Estimation of the amount of retained austenite in austempered ductile irons

Austempered ductile irons usually contains a large quantity of retained austenite that can help to optimise their mechanical properties. Therefore, the maximisation of retained austenite is very important. This can be achieved by modifying the composition and heat treatment of the steel: for example, carbon and silicon contents play an important role as well as austempering time and temperature. The problem of designing these cast irons involves many variables and considerable complexity which can only be represented by a neural network.

In this study, a neural network has been used to estimates the maximum volume fraction of retained austenite in a basic cast iron (Fe-3.5C-2.8Si-0.25Mn-0.25Mo-0.5Cu wt%). The input parameters for the neural network were:

Input element	Minimum	Maximum	Mean	Standard deviation
Carbon (wt.%)	2.3	3.97	3.58	0.165
Silicon (wt.%)	1.57	3.78	2.57	0.21
Manganese (wt.%)	0.01	1.52	0.34	0.23
Molybdenum ^a (wt.%)	0.0	0.74	0.16	0.17
Nickel ^a (wt.%)	0.0	3.82	0.29	0.53
Copper ^a (wt.%)	0.0	1.60	0.23	0.29
Austenitising temperature (°C)	800	1050	900	34
Austenitising time (min)	15	240	97	34
Austempering temperature (°C)	230	455	350	39
Austempering time (min)	0.5	60000	1039	5625
Austempering time $\ln \{t_A/s\}$	1.477	6.556	3.659	0.948
$\ln \{-\ln \{V_\gamma\}\}$	-0.875	2.03	0.414	0.418

Figure 1: Input parameters used in the neural network

A few results produced by the neural network are given. Figure 3 shows the prediction of the volume fraction as a function of carbon and silicon:

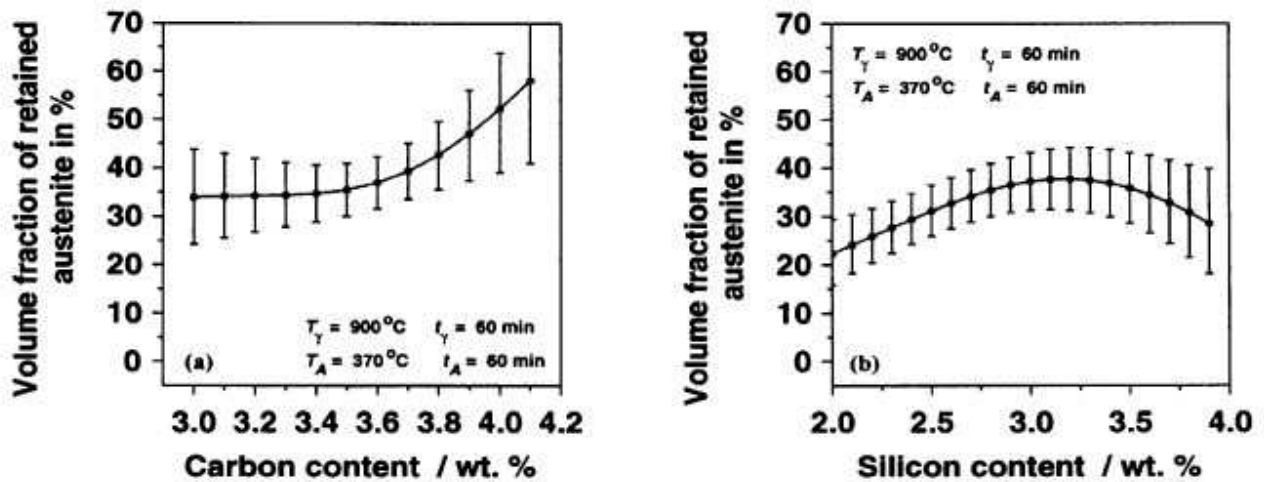


Figure 2: Predicted values for retained austenite

According to the prediction, the volume fraction of retained austenite hardly changes as the carbon concentration increases from 3.1 to 3.7 wt%. As for silicon, the volume fraction increases from 2 to 3.2 wt% and then decreases, the optimal concentration being 3.2 wt%. This is in agreement with what has been reported in the literature. Concentration from 2.5 to 3.1 wt% allow for more bainitic transformation and consequently more austenite carbon enrichment without precipitation of carbon. Above the optimal value, it has been reported that the drop in

the volume fraction is caused by the formation of islands of pro-eutectoid ferrite in the bainite structure.

Figure 3 shows the prediction of the volume fraction as a function of nickel and copper:

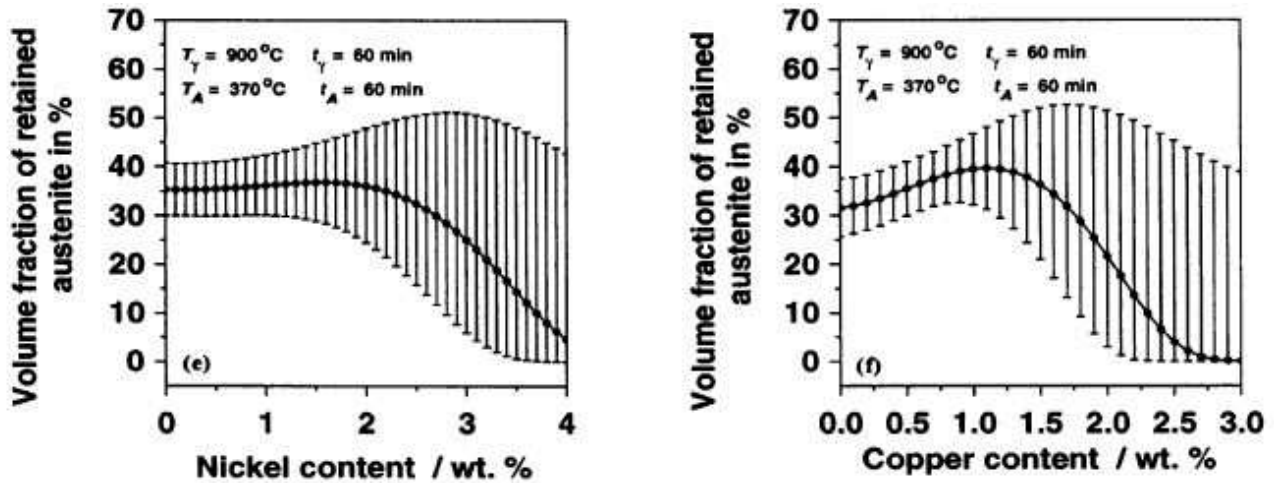


Figure 3: Notice that the calculated fraction is confined to between 0 and 1.

In this case, when the concentration of nickel and copper is respectively below 2 and 1.25 wt%, the prediction can be reliable. In the first case, the volume fraction of retained austenite does not seem to be influenced by the nickel concentration. In the second case, copper stabilises austenite and leads to a greater fraction of retained austenite. But above those limits (2 wt% for Ni and 1.25 wt% for Cu), the model can no more be trusted and this is inferred by the large error bars. More experiments with concentrations in this range of values need to be carried out to improve the model. Uncertainty because of a lack of data is one of the limitations of a neural network.

4 Second example: Modelling of creep strength of austenitic stainless steels

Austenitic stainless steel are commonly used in the power industry at temperatures greater than 650°C and stresses of 50 MPa or more and are expected to remain in service for more than 100 000 hours. Such time periods are not accessible experimentally and long-term properties need to be extrapolated from shorter term tests. Empirical expressions have been developed to express the creep stress rupture as a function of the chemical composition. Equation 1 for

example was proposed for the 10^4 h creep rupture stress ($\sigma_{f,10^4h}$) of an AISI 316 steel at 650°C:

$$\sigma_{f,10^4h} = 173.8 + 7243[B] + 961.1[N] + 1145[S] - 7.5[Cr] \quad (1)$$

The main problem is that different equations might be needed for different alloys at different temperatures. Moreover, these models only take in account the role of a few alloying element and seldom take in account interactions between those elements. To overcome this problem, a neural network model is the solution.

In this example, the output parameter is the 10^4 h creep rupture stress ($\sigma_{f,10^4h}$) and the input parameters are presented in Figure 4:

Input variable	Min.	Max.	Mean	Standard deviation
Test stress, MPa	5	443	145	72
Test temperature, °C	500	1050	667	71
Log (rupture life, h)	- 0.200	5.240	3.324	0.879
Composition, wt-%				
Cr	12.98	22.22	18.08	1.35
Ni	8.40	32.48	13.82	5.47
Mo	0.00	2.82	1.05	1.10
Mn	0.56	2.50	1.36	0.35
Si	0.040	1.150	0.545	0.171
Nb	0.000	2.980	0.242	0.449
Ti	0.000	0.560	0.131	0.199
V	0.000	0.090	0.004	0.011
Cu	0.000	0.310	0.051	0.074
N	0.000	0.170	0.029	0.052
C	0.012	0.330	0.062	0.025
B	0.000	0.005	0.001	0.0016
P	0.000	0.038	0.021	0.0067
S	0.000	0.030	0.012	0.0071
Co	0.000	0.540	0.037	0.1090
Al	0.000	0.520	0.029	0.0804
Solution treatment temperature (°C)	1000	1350	1102	51

Figure 4: Input parameters used in the neural network

Some results are given below. Figure 6 gives the evolution of $\sigma_{f,10^4h}$ as a function of the chromium and boron content.

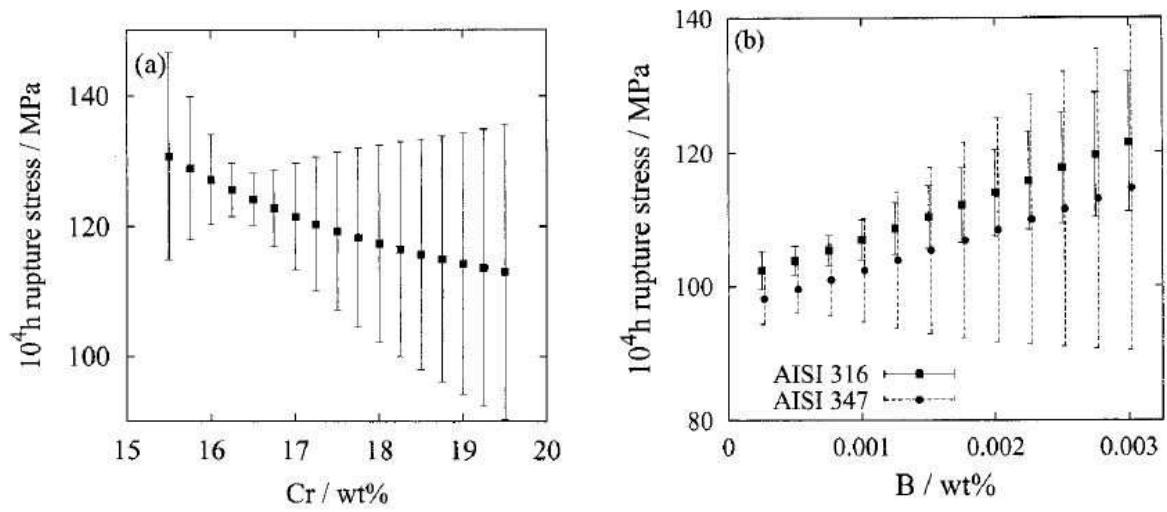


Figure 5: Predicted values for Cr and B

Cr reduces the creep rupture strength, which is in agreement with equation 1 but the mechanism is not, so far, understood. As for boron, the model predicts that it has a strong effect on $\sigma_{f,10^4h}$, increasing the value from 100 to ≈ 120 MPa. This was emphasised by the large value of the coefficient (7243) in equation 1.

Figure 6 compares the neural network prediction with other prediction methods and with experimental values.

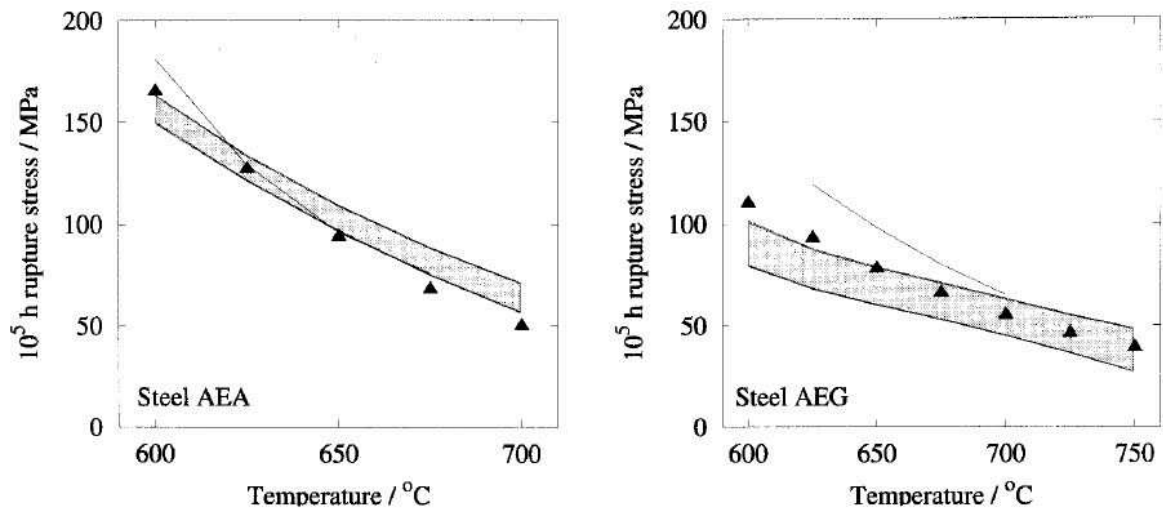


Figure 6: Comparison of prediction methods

The neural network prediction is the shaded area, a prediction using another method (Orr-Sherby-Dorn method) used by the National Research Institute for Metals is represented by a line and recent experimental data are represented by a triangle. The agreement with experimental data is good, particularly in the case of steel AEG where the neural network gives significantly better predictions than the Orr-Sherby-Dorn method. In this case, a neural network, without taking in account any mechanisms or microstructure changes gives better results than a model based on theory.

5 Third example: Modelisation of irradiation hardening in low-activation steels

Fusion power plants, based on a plasma of deuterium and tritium, are expected to be the next source of power but the design of material used for the magnetic confinement remains the main problem. 14 MeV neutrons that escape from the plasma will damage the first wall of the confinement. Defects (such as vacancies, interstitials, microvoids filled with helium or precipitates) produced during the lifetime service will embrittle and harden the material.

The design of such material should rely on a database of measured mechanical properties of candidate fusion materials. However, there are few data for materials at high damage dose which can be found in a fusion environment. Thus, properties have to be estimated and extrapolated from data already available. A neural network is, in this case, suitable to establish relations between inputs parameters and the yield strength (Y_s). Figure 7 lists the parameters that were used in the model:

Input variable	Min.	Max.	Mean.	Standard deviation
Irradiation temperature, T_{irr} , K	273	925	401.2	179.3
Test temperature, T_{test} , K	123	973	549.5	209.4
Dose, dpa	0	90	3.47	10.04
He content, appm	0	5000	38.4	359.8
Cold working, %	0	10	0.09	0.94
Composition, wt%				
C	0.087	0.2	0.097	0.013
Cr	2.25	12	8.325	1.027
W	0	3	1.485	0.778
Mo	0	1	0.16	0.363
Ta	0	0.54	0.064	0.102
V	0	0.3	0.182	0.054
Si	0	0.37	0.055	0.052
Mn	0	1.13	0.145	0.204
N	0	0.06	0.0025	0.081
Al	0	0.054	0.0008	0.037
As	0	0.005	0	0.0003
B	0	0.0085	0.0007	0.0013
Bi	0	0.005	0	0.0003
Ce	0	0.036	0.0001	0.0022
Co	0	0.01	0.0002	0.0009
Cu	0	0.035	0.0006	0.0032
Ge	0	1.2	0.0139	0.128
Mg	0	0.01	0	0.0006
Nb	0	0.16	0.0017	0.011
Ni	0	2	0.0576	0.31
O	0	0.009	0.0002	0.0011
P	0	0.007	0.0013	0.0014
Pb	0	0.005	0	0.0003
S	0	0.005	0.0012	0.0011
Sb	0	0.003	0	0.0002
Se	0	0.003	0	0.0002
Sn	0	0.003	0	0.0002
Te	0	0.005	0	0.0003
Ti	0	0.25	0.0099	0.046
Zn	0	0.005	0	0.0003
Zr	0	0.059	0.0003	0.0036

Figure 7: Input parameters used in the neural network

Predictions given with a neural network were in agreement with the general trend reported in the literature and with some experimental values. It is well-known that irradiation-induced hardening saturates with fluence. Figure 8 illustrates this trend for Eurofer'97 (0.1C-9Cr-1.1W-0.15Ta-0.2V). Y_s increases from 450 MPa to 650 MPa, reaches a maximum at 10 dpa and then slowly decreases (in other conditions, Y_s still continues to increase but the rate of increase decreases).

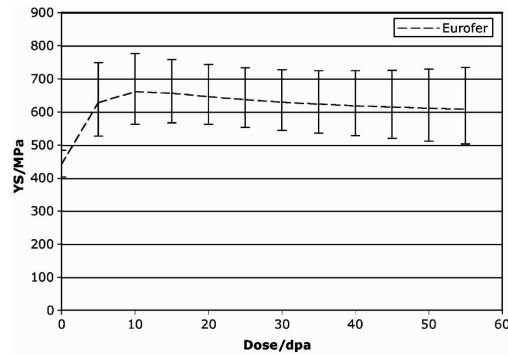


Figure 8: Model predictions for Eurofer 97

Figure 9 gives a prediction of the behaviour of a modified F82H steel whose composition is (in wt%) 0.09C-7.7Cr-1.94W-0.02Ta-0.016V-0.11Si-0.016Mn-0.0002B-0.002P-0.002S. On the same graph are also plotted some experimental values.

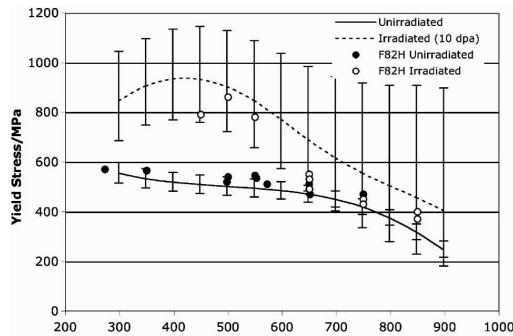


Figure 9: Model predictions for F82H compared to experimental values

The model gives relatively good predictions for unirradiated steels but for irradiated steels, experimental values are slightly below the prediction but within the error bars.

6 Fourth example: Modelisation of ferrite number in austenitic stainless steel welds

The ferrite content in stainless steel plays an important role in determining the fabrication and service performance of welded structures. Several properties of stainless welded steels can be predicted by estimating the ferrite content. A minimum ferrite content is necessary to ensure hot cracking resistance whereas an maximum content limit determines the propensity to embrittlement due to second phase. Several diagrams have been designed to estimate the content of ferrite but they all are based on linear or pseudo-linear relations and do not take in account every chemical component, interactions between them or changes in the microstructure. Those problems can be overcome by a neural network. In this case, input parameters that were used to train the model are presented in figure 10:

Elements	Minimum	Maximum	Mean	Std. Deviation
C	0	0.2	0.04	0.0219
Mn	0.35	12.67	1.88	1.79
Si	0.03	6.46	0.53	0.35
Cr	1.05	32	20.51	2.76
Ni	4.61	33.5	11.31	2.56
Mo	0.01	10.7	1.42	1.64
N	0.01	2.13	0.09	0.14
Nb	0	0.88	0.03	0.098
Ti	0	0.33	0.02	0.028
Cu	0	6.18	0.14	0.437
V	0	0.23	0.04	0.04
Co	0	0.69	0.03	0.046
Fe	45.59	72.51	63.94	4.33
FN	0	98	12.04	17.31

Figure 10: Input parameters used in the neural network

The composition of 308 L in wt% is given in Table 1 and examples of predictions are given in Figures 11, 12 and 13 :

Table 1: Composition of 308 L in wt%

C	Mn	Si	Cr	Ni	Mo	N	Nb	Ti	Cu	V	Co
0.035	0.08	0.4	20.4	10	0.05	0.06	0.07	0.08	0.14	0.09	0.07

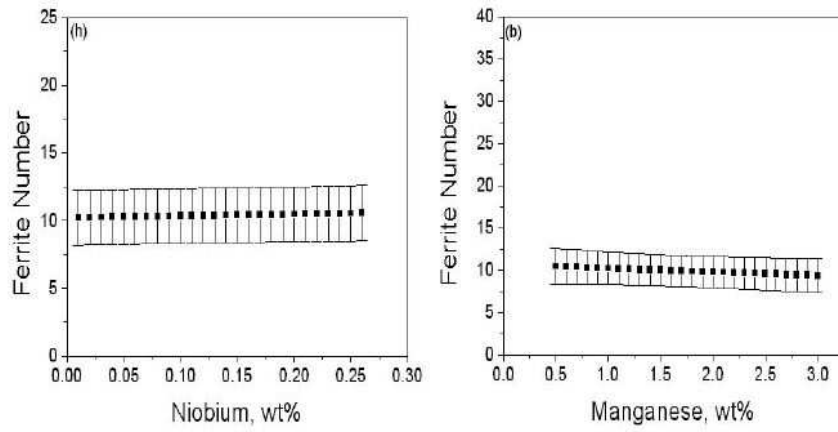


Figure 11: Predicted values for 308 L

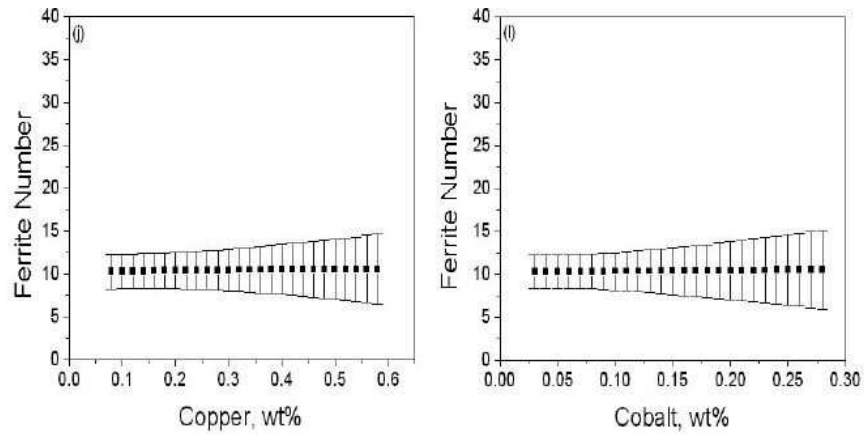


Figure 12: Predicted values for 308 L

Figures 11 and 12 show that the variation in elements like Ni, Mn, Cu or Co are found not to influence the ferrite content for this basis composition.

Figure 13 presents the variations of the ferrite number as a function of nickel and chromium. The addition of nickel reduces the content of ferrite, indicating that it is a strong austenite stabiliser whereas chromium is a strong ferrite stabilizer

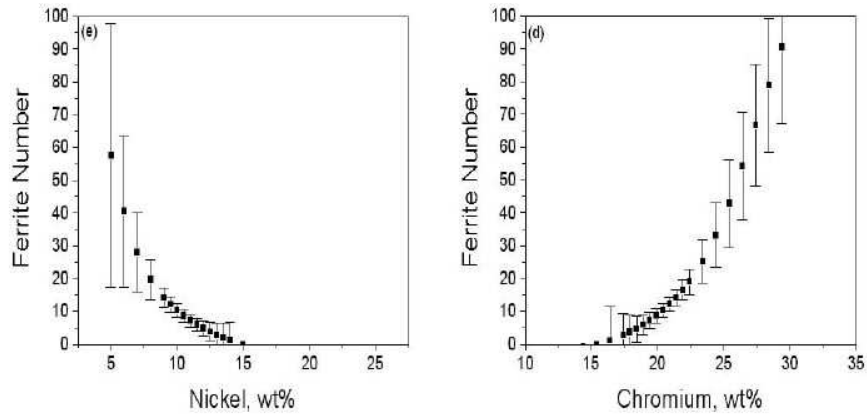


Figure 13: Predicted values for 308 L

This can be linked to Figure 14 which gives the significance of every input parameter:

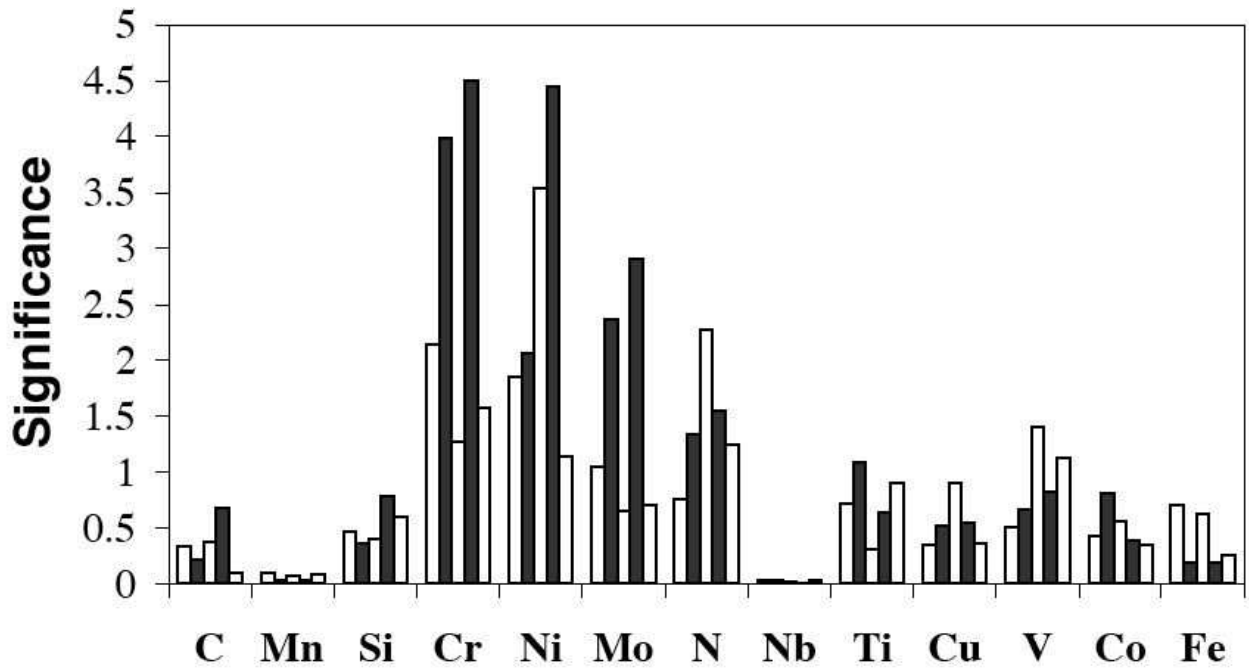


Figure 14: Significance of input parameters

Elements such as Ni, Mn, Cu or Co, which do not influence the ferrite number, have a low significance (between 0 and 0.5) whereas elements which have a strong influence (as an austenite or ferrite stabilizer) have a higher significance (up to 4.5 for Ni and Cr).

7 Conclusion

Building a neural network is relatively easy. The software calculates everything, orders sub-models according to their performances and finds the best combination to build the model. This is done in a few hours depending on the size of the database and the power of the computer. But the difficulty in obtaining accurate predictions in agreement with experimental data remains the preparation of the database, the choice of appropriate parameters, the introduction of artificial parameters that would help the network to discover complex non-linear relations.

When this process has been carefully realised, a neural network is indeed a powerful tool to established relations between parameters and a physical properties. The four examples described earlier showed that a NN can represent the general trend in the evolution of a properties. When compared to experimental data, it is in relative agreement but those examples also reveal the limits of a neural network. The accuracy of a NN mainly depends on the size and precision of the database. A database containing an insufficient number of samples will not give good predictions. A weak knowledge of the physics and theory of the studied problem will lead to a bad choice of parameters and predictions. Data which do not cover the range of parameters will give bad predictions (predictions with big error bars) where the data are sparse.

References

- [1] M. A. Yescas, H. K. D. H. Bhadeshia, and D. J. MacKay. Estimation of the amount of retained austenite in austempered ductile irons. *Materials Science and Engineering*, A311:162–173, 2001.
- [2] H. K. D. H. Bhadeshia T. Sourmail and D. J. C. MacKay. Neural network model of creep strength of austenitic stainless steels. *Materials Science and Technology*, 18:655–663, 2002.
- [3] R. Kemp, G.A. Cottrell, H.K.D.H. Bhadeshia, G.R. Odette, T. Yamamoto, and H. Kishimoto. Neural-network analysis of irradiation hardening in low-activation steels. *Materials Science and Technology*, 348:311–328, 2006.
- [4] M. Vasudevan, M. Muruganath, and A. K. Bhaduri. Application of bayesian neural network for modeling and prediction of ferrite number in austenitic stainless steel welds. In H. Cerjak and H. K. D. H. Bhadeshia, editors, *Mathematical Modelling of Weld Phenomena - VI*, pages 1079–1100. Institute of Materials, 2002.